A Reconfigurable Notched Band Monopole Antenna for C-Band Applications

Samar A. Refaat[1], Hesham A. Mohamed[2], Abdelhady M. Abdelhady[1], and Ashraf S. Mohra[1]
[1] Electrical Engineering Department, Benha Faculty of Engineering, Benha University, Benha, Egypt
[2] Microstrip Department, Electronics Research Institute (ERI), Cairo, Egypt
Email: {samar.rafaat, amohra}@bhit.bu.edu.eg; hesham_280@eri.sci.eg; abdoeng78@gmail.com

***Abstract*—In this paper, a wideband monopole antenna with reconfigurable frequency notch through wireless local area network (WLAN) (5.15-5.35GHz and 5.725-5.825GHz) or future wireless fidelity 6GHz (Wi-Fi-6E) (5.925-7.125GHz) band for C-band applications is presented. The conventional/basic monopole antenna consists of four-leaf clover antenna structure with cascaded feeder and Defected Ground Structure (DGS). The basic antenna is designed and then simulated using Computer Simulation Technology (CST) and High-Frequency Structure Simulator (HFSS) readymade software programs. The antenna covering an operational bandwidth extends from 4.2GHz to 9.2GHz while the gain is around 4.0dBi. Two simple resonator conductors are added near the thin feeder of antenna to realize the notched frequency. The rejected frequency within WLAN or Wi-Fi 6E bands is controlled by the resonator conductor lengths, so Positive-Intrinsic-Negative (PIN) diodes switches are inserted to achieve the required length for each rejected band. Finally, each of the basic antenna and the proposed notched antenna are fabricated and measured. The measurement results are in good agreements with the simulated results of CST and HFSS, providing good antenna performance and sharp notches with good rejection values.**

***Index Terms*—Wideband monopole antenna, WLAN/Wi-Fi 6E, rejected frequency, PIN diodes, reconfigurable, C-band applications**

I. Introduction

It is essential to prevent overlapping and interfering between Ultra-Wideband (UWB) system and wireless communication systems like WLAN as it causes signal distortion and decreasing antenna sensitivity. Band-notched antennas were designed to get over the interference and avoid signal distortion. Different techniques and approaches were improved to design these antennas, including etching slots in radiating patch or ground [1]-[8], adding parasitic elements and using stubs [9]-[13]. In most of these works, the notched band selectivity was not very good as the overall entire band (5-6GHz) was rejected not the specified WLAN bands (5.15-5.35GHz and 5.725-5.825GHz). This means that any desirable data between lower and upper WLAN band (5.35-5.725GHz) will be lost. Consequently, it causes a bad impact on the signal and degrades the signal quality. Another limitation in these approaches is that WLAN notch is always active regardless the interference band exists or not. Also, in [12] and [13], each of antenna size, complexity and cost increased due to the integration of filters and resonators to the basic antenna. To avoid rejection of entire WLAN band, an efficient antenna with two sharp notches of lower and upper WLAN bands was realized by using independent controllable strips in [14]. In [15], three rejection bands at 3.3-4.0GHz, 5.15-5.4GHz, and 5.8-6.1GHz (WiMAX and WLAN bands) were realized by complementary split ring resonators (CSRRs) and DGS. Switchable/reconfigurable band notches in UWB antennas were designed using switchable structures, PIN diodes, varactors and switches to solve the problem of permanent presence of rejected band and design more efficient antenna. In [16], five PIN diodes were used in the main patch to achieve switchable band notches for WiMAX or WLAN notch. In [17], two open ended slots were inserted in the ground as two notch filters to control notched frequencies at WiMAX and WLAN bands. In [18], a reconfigurable slot antenna was designed with two strip lines and two diodes to reject WiMAX or WLAN band or both bands. Also, an improved gain antenna with etched structure in the main patch with lumped capacitor for changing the notch frequency from WLAN to WiMax band was discussed in [19]. In [20], reconfigurable dual band notches at 3.8GHz and 5.5GHz were realized by using two electronic switches within the SRR and CSSRR of the antenna structure. Also, dual tunable notched band at 3GHz and 6.8GHz was discussed in [21], two varactor diodes were used on the CSRR rings to control notch frequencies. In [22], triple notch bands like WLAN, WiMax and some of the x-band applications were realized by pin diodes in the ground plane with small shifting in the notched bands according to the diodes ON/OFF states. In [23], the WiMax band was rejected by placing a slot resonator in the main antenna radiator, while the WLAN notch was controlled by variable capacitors in the inverted L-shaped resonator.

In April 23, 2020, the Federal Communication Commission (FCC) in the USA has ruled that 1200 megahertz (5.925-7.125GHz) of spectrum in the 6GHz band available for unlicensed use. These new rules will be included in the next generation of WiFi (Wi-Fi 6) playing an important role in the growth of IoT [24], [25]. Traditionally, WiFi technology including Wi-Fi 6 used 2.4GHz and 5GHz bands, so this new frequency band

Manuscript received March 23, 2021; revised May 2, 2021; accepted May 28, 2021.
Corresponding author: Samar A. Refaat (email: samar.Rafaat@bhit.bu.edu.eg)

doi: 10.18178/ijeetc.10.6.389-396

will support WiFi technology to operate with high data rate, high throughput, high performance and lower latency. This means that the new WiFi-6E uses the capabilities of 6GHz to enable high-bandwidth applications that require faster data throughput like streaming video in HD, and online or virtual reality gaming. It'll also allow businesses valuable options for the expansion of their networks and networking devices.

In this paper, a new printed wideband monopole antenna with different switchable rejection bands is designed, fabricated and measured. Two resonator conductors are designed far from the basic monopole antenna structure and beside the thin feeder of the antenna with a group of PIN diodes to control conductor length for tuning notch frequency in WLAN (5.15-5.35GHz and 5.725-5.825GHz) or WiFi-6E (5.925–7.125 GHz) band. The proposed antenna is suitable for C-band applications with no interferences by Wi-Fi 6E or WLAN services. The antenna is analyzed and simulated with the help of CST and HFSS software programs, then fabricated and measured. The antenna parameters such as return loss, antenna gain, radiation patterns and surface current distribution are analyzed producing overall good performance with sharp notches at good rejection values.

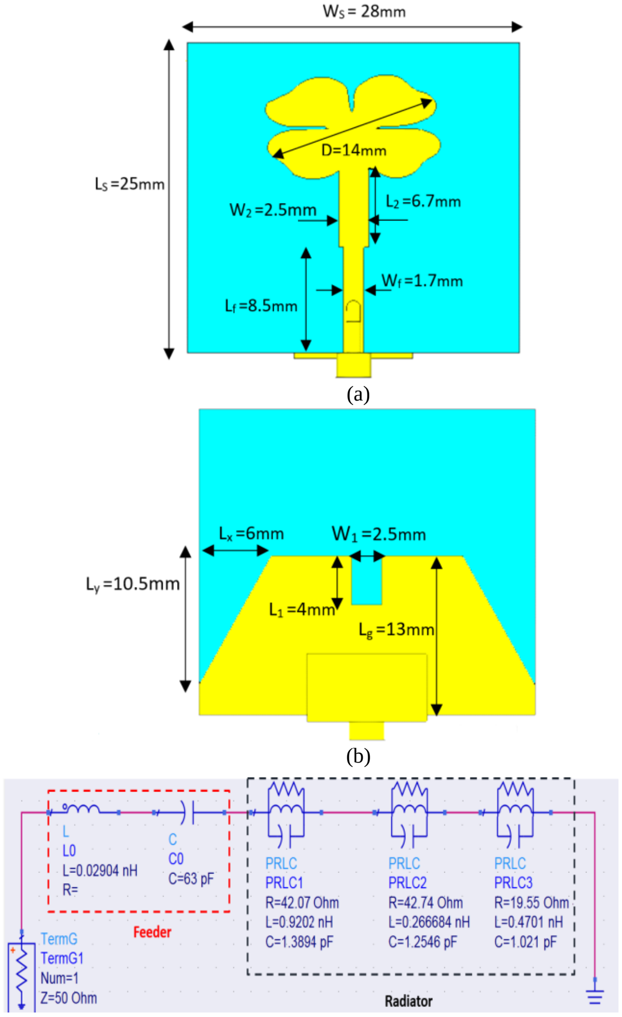

Fig. 1. A four-leaf clover wideband antenna: (a) Top layer, (b) bottom layer, and (c) equivalent circuit model.

In Section II, the design and analysis of the basic wideband antenna is described. Also, parametric study of some of antenna parameters is presented in Section III. In Section IV, the proposed wideband monopole antenna with reconfigurable notched band characteristics with simulation results are illustrated. Section V discusses the fabrication of antennas and simulation vs measurement results. Finally, conclusion of this work is provided in Section VI.

II. Design and Analysis of Basic Wideband Monopole Antenna

The layout and equivalent circuit model of the proposed four-leaf clover wideband monopole antenna are shown in Fig. 1, the idea of this structure is based on [26]. The presented monopole antenna is designed and fabricated on Roger/Duroid-4003C substrate (ε_r=3.38, h=0.81mm and tanδ=0.001). Some modifications were done on clover antenna-1 to antenna-2 and its simulation result is shown in Fig. 2 with (S_{11})<–10dB, a rectangular slit in the ground plane is etched in antenna-2 to improve the impedance matching as seen in Fig. 2.

In antenna-3, the ground plane was truncated to improve lower frequency band selectivity and impedance matching. The proposed antenna, Fig. 3 is simulated using two software packages CST and HFSS, while the ADS simulator was used for the equivalent circuit model. The simulated reflection coefficient $|S_{11}|$ shows that the impedance bandwidth extends from 4.2GHz to 9.2GHz with fractional bandwidth (FBW)greater than 74.63% as shown in Fig. 3. Fig. 4 displays the monopole antenna surface current distribution where the radiation is around the antenna structure and some edges of the feeder. Also, simulated antenna average gain and efficiency is around 4dBi and 98%, respectively as plotted in Fig. 5. Furthermore, simulated radiation patterns are depicted in Fig. 6, showing E-plane, and H-plane radiation patterns that give nearly omnidirectional and stable on the entire passband.

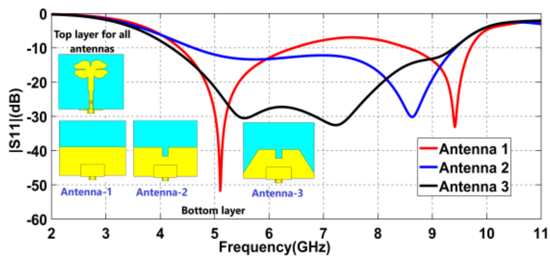

Fig. 2. Development of the antenna structure with simulated results of return loss $|S_{11}|$.

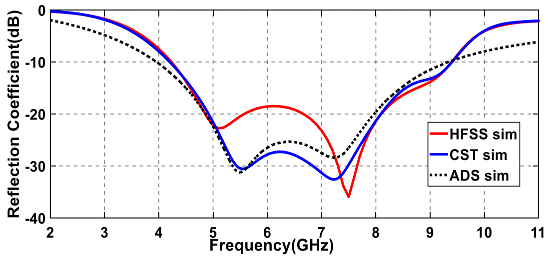

Fig. 3. Simulated $|S_{11}|$ for antenna 3.

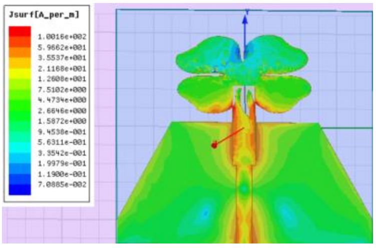

(a)

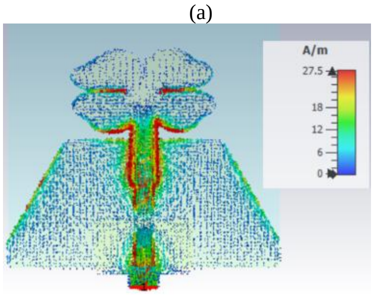

(b)

Fig. 4. Surface current distribution for wideband monopole antenna by a) HFSS b) CST.

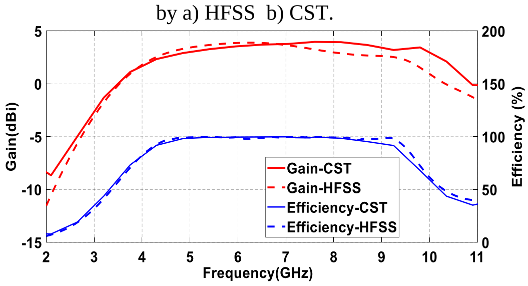

Fig. 5. Simulated wideband monopole antenna gain and efficiency.

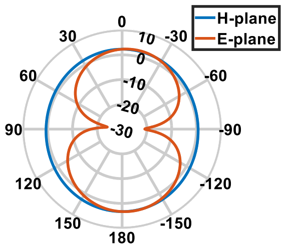

(a)

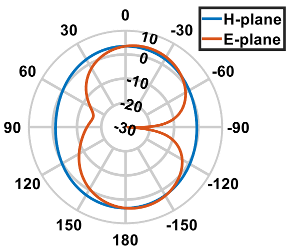

(b)

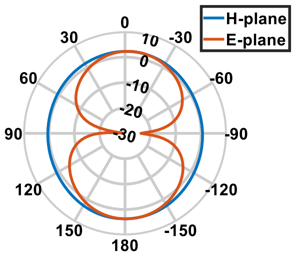

(c)

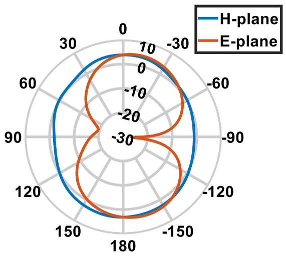

(d)

Fig. 6. Simulated radiation patterns for wideband antenna by CST at: (a) 5.5 GHz, (b) 7.5GHz and by HFSS at c) 5.5, and d) 7.5 GHz.

III. Parametric Study of the Wideband Antenna

A parametric study is carried out studying the four -leaf clover wideband monopole antenna, Fig. 1 (a) and (b) to get the best performance.

A. Ground Rectangular Slit Length (L_1)

Taking the antenna-2 as the reference antenna, a slit is etched with constant width W_1=2.5 mm and slit length L_1 is varied to optimize the performance. Fig. 7 (a) illustrates the $|S_{11}|$ response with different slit length (L_1) values. The length L_1=4mm gives the optimum performance (S_{11}<–10dB) and has a reasonable roll-off (–4.7dB/GHz) compared with other lengths at the start frequency and a good rollup (16.9dB/GHz) at the end frequency.

B. Ground Truncated Dimensions (L_x, L_y)

With using the length L_1=4mm, the dimensions L_x, L_y of truncated ground are varied until reached to the optimum values L_x=6mm and L_y=10.5mm that give the better performance for return loss, Fig. 7 (b).

C. Ground Length (L_g)

The parameter L_g basically affects $|S_{11}|$ response and antenna operating bandwidth as described in Fig. 7 (c). For the chosen L_g lengths, the frequencies near the start of the operating bandwidth are nearly the same, but the upper frequency is changed. The best operating band-width performance is realized at optimum L_g=13mm.

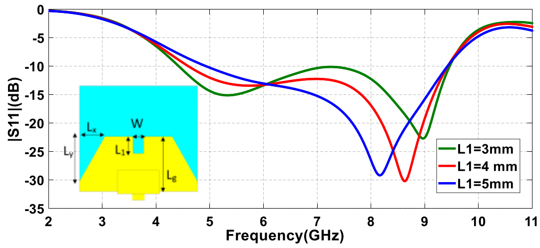

(a)

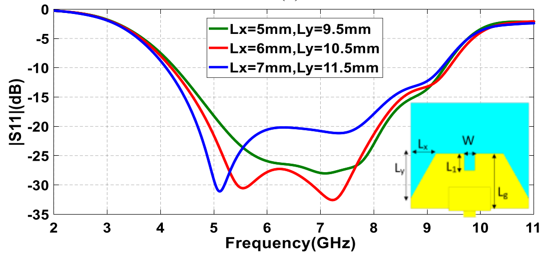

(b)

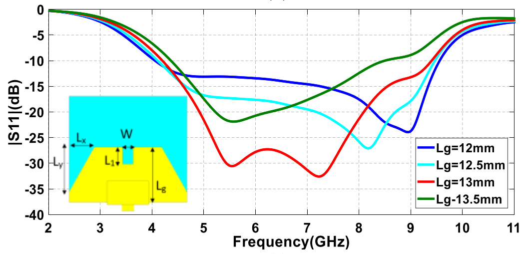

(c)

Fig. 7. Reflection coefficient $|S_{11}|$ of wideband monopole antenna against (a) the slit length (L_1). (b)Truncated ground (L_x, L_y). (c) Ground length (L_g).

IV. Proposed Notched Antenna Simulation Results

Two simple resonator conductors are added near the thin antenna feeder, as seen in Fig. 8, to control the frequency notch inside WLAN or Wi-Fi 6E band. When the resonator conductor length varied from 16 to 22 mm, the rejected frequency will be varied inside the band from 5 to 7GHz which covers WLAN and Wi-Fi 6E bands as shown in Fig. 9. It is clear that, the notch frequency is inversely proportional to overall conductor, Fig. 10. An empirical formula based on the second order polynomial equation is deduced by at least square method [27] to get the relation between the rejected frequency and the resonator conductor length with error not exceed ±1.7%:

$$F_{notch}=0.0198L^2-1.1068L+19.80 \quad (1)$$

where F_{notch} in GHz is corresponding the rejected frequency and L in mm represents the overall resonator conductor.

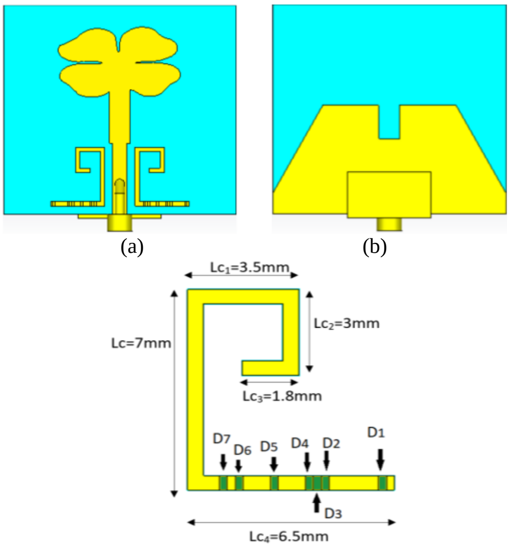

Fig. 8. The structure of proposed notched band antenna: (a) Top layer, (b) bottom layer, and (c) resonator conductor dimensions.

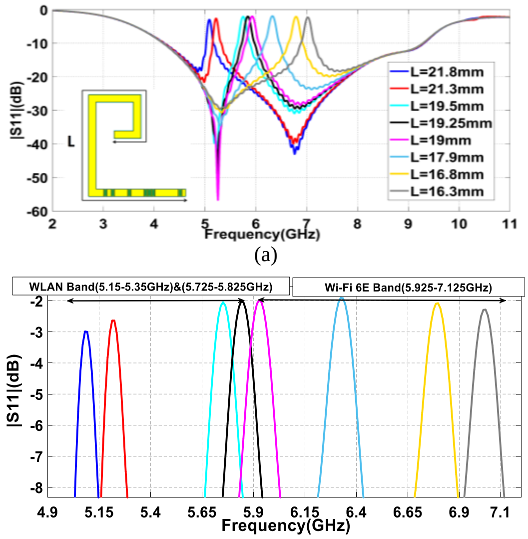

Fig. 9. The proposed antenna: (a) Variation of return loss $|S_{11}|$ against conductor length and (b) Focus on rejected frequencies.

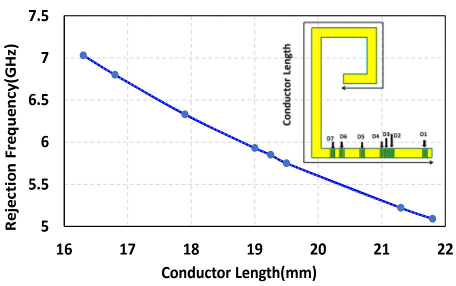

Fig. 10. The rejected frequency versus resonator conductor length.

To explain the effect of resonator conductors on the passband and how the rejected band is realized, simulated current distribution at the first rejected band frequency (F_{notch}=5.09GHz, L=21.8mm) is described in Fig. 11. At this frequency, the current distribution is around the edges of resonator conductors and nearly no current is distributed around the antenna. Since, the resonator conductor length controls the rejected frequency, seven PIN diodes (D1 to D7), Fig. 10 can be used to control the variation of resonator conductor length, where the ON/OFF states for diodes are controlled by a diodes switch matrix box (USB-8SPDT-A18) that operates over a wide frequency band from DC to 18 GHz.

Table I illustrates the states for diodes, resonator conductor length, the corresponding notch frequency, and the corresponding return loss $|S_{11}|$ value using CST and HFSS software simulators. The simulated return loss results are shown in Fig. 12 (a) and Fig. 12 (b) for each of WLAN and Wi-Fi 6E bands. The deviation between the two simulators results is due to using two different numerical techniques. Simulated results show sharp notches with good rejection values at each notch in WLAN band or Wi-Fi 6E band. The simulated notched antenna gain and efficiency for all stopbands are given in Fig. 13 and Fig. 14 showing that gain and efficiency in the rejected bands fall to less than –4.5dB and 25%, respectievely. Also, notching structures decrease the gain within maximum FBW (1.49%) at f=7.03 GHz, Fig.12.

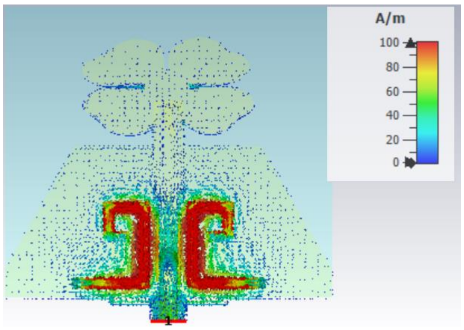

Fig. 11. The Surface current distribution at F_{notch}=5.09GHz.

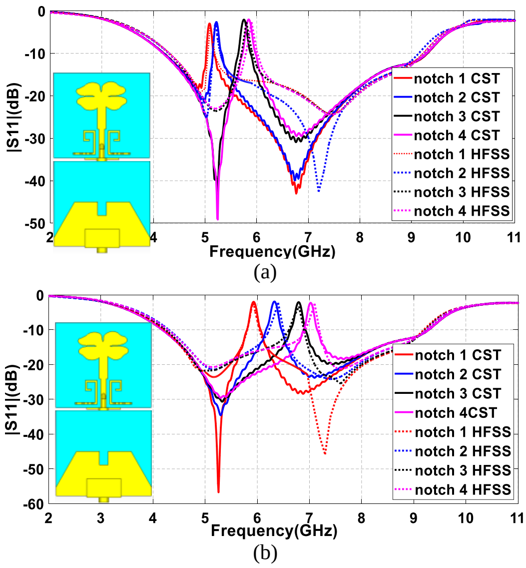

Fig. 12. The proposed antenna simulated return loss $|S_{11}|$ (a) in WLAN band; (b) in Wi-Fi 6E band.

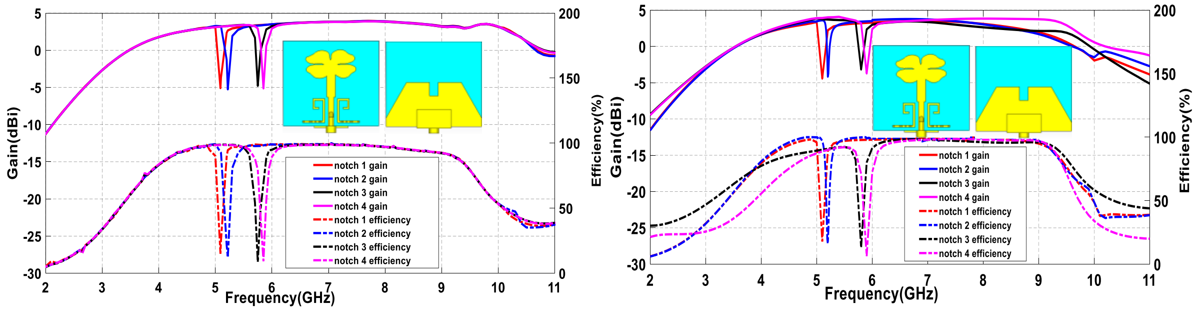

Fig. 13. The proposed antenna simulated gain and efficiency for WLAN notch states by a) CST b) HFSS.

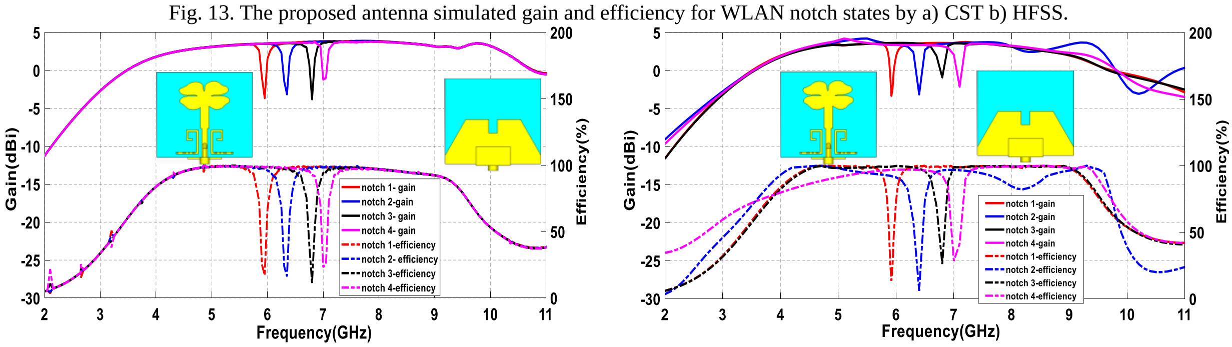

Fig. 14. The proposed antenna simulated gain and efficiency for Wi-Fi 6E notch states by a) CST b) HFSS.

TABLE I: DIODES GROUP STATES AND ITS CORRESPONDING NOTCH FREQUENCY IN WLAN BAND (5.15–5.35GHZ & 5.725-5.825GHZ) AND WI-FI 6E BAND (5.925 -7.125GHZ).

Notch number	Resonator conductor length (mm)	D1	D2	D3	D4	D5	D6	D7	CST Results F_notch (GHz)	CST Results S_{11}(dB)	HFSS Results F_notch (GHz)	HFSS Results S_{11}(dB)
WLAN Notches (5.15–5.35GHz & 5.725-5.825GHz)												
1st notch	21.8	ON	ON	ON	ON	ON	ON	ON	5.09	-3	5.1	-3.16
2nd notch	21.3	OFF	ON	ON	ON	ON	ON	ON	5.22	-2.64	5.2	-3
3rd notch	19.5	OFF	OFF	ON	ON	ON	ON	ON	5.75	-2.06	5.8	-2.65
4th notch	19.25	OFF	OFF	OFF	ON	ON	ON	ON	5.85	-2.04	5.9	-2.64
Wi-Fi 6E Notches (5.925 -7.125GHz)												
1st notch	19	OFF	OFF	OFF	OFF	ON	ON	ON	5.93	-1.98	5.92	-2.46
2nd notch	17.9	OFF	OFF	OFF	OFF	OFF	ON	ON	6.33	-1.91	6.4	-2.26
3rd notch	16.8	OFF	OFF	OFF	OFF	OFF	OFF	ON	6.8	-2.09	6.8	-3.31
4th notch	16.3	OFF	OFF	OFF	OFF	OFF	OFF	OFF	7.03	-2.29	7.1	-2.54

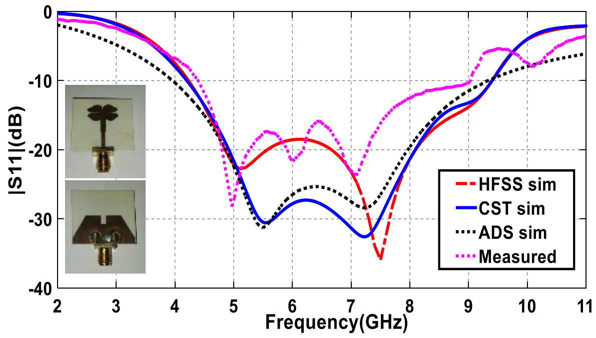

Fig. 15. Simulated, equivalent circuit model and measured reflection coefficient results for wideband antenna.

V. MEASUREMENT RESULTS AND COMPARISON

The wideband monopole antenna and proposed antenna with switchable band rejections are fabricated then measured using the vector network analayzer, Fig. 15 shows simulated and measured $|S_{11}|$ results for wideband antenna without resonator conductor showing a small difference in measured results due to fabrication tolerance and SMA connector mismatch. Fig. 16 refers to the antenna with two resonator conductors connected to a USB RF Switch Matrix (USB-8SPDT-A18) photograph.

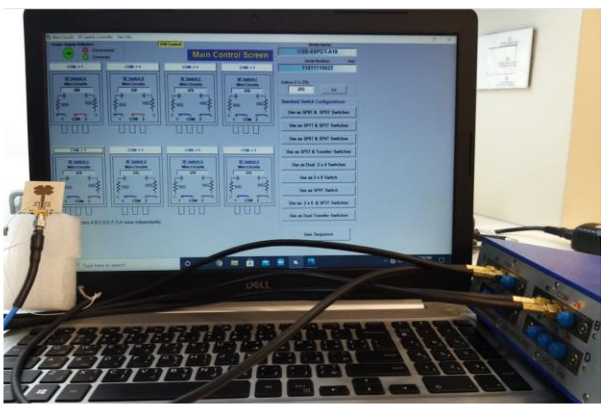

Fig. 16. The proposed notched antenna with a diodes switch matrix box (USB-8SPDT-A18) photograph.

The measured and simulated $|S_{11}|$ for the proposed antenna for first WLAN notch and fourth Wi-Fi 6E notch are shown in Fig. 17 (a) and Fig. 17 (b) while Fig. 17 (c) show the antenna equivalent circuit model [28] for the first WLAN and fourth WiFi-6E notches. The ADS results are in good agreement with HFSS/CST simulator results with average deviation ±3.7dB within the operating bandwidth. Due to the unavailability of measurement facilities of the radiation pattern, the two different simulators CST and HFSS are used to give the radiation pattern analysis, where CST software is based on FIT method (finite integral technique) while HFSS uses FEM (finite element method). The simulated radiation patterns for E and H- planes for 1st notch and 4th notch in WLAN and WiFi 6E band, respectively are illustrated in Fig. 18 showing that no radiation at these frequencies. Finally, a comparison between the existing literature of the antenna and the proposed antenna is listed in Table II.

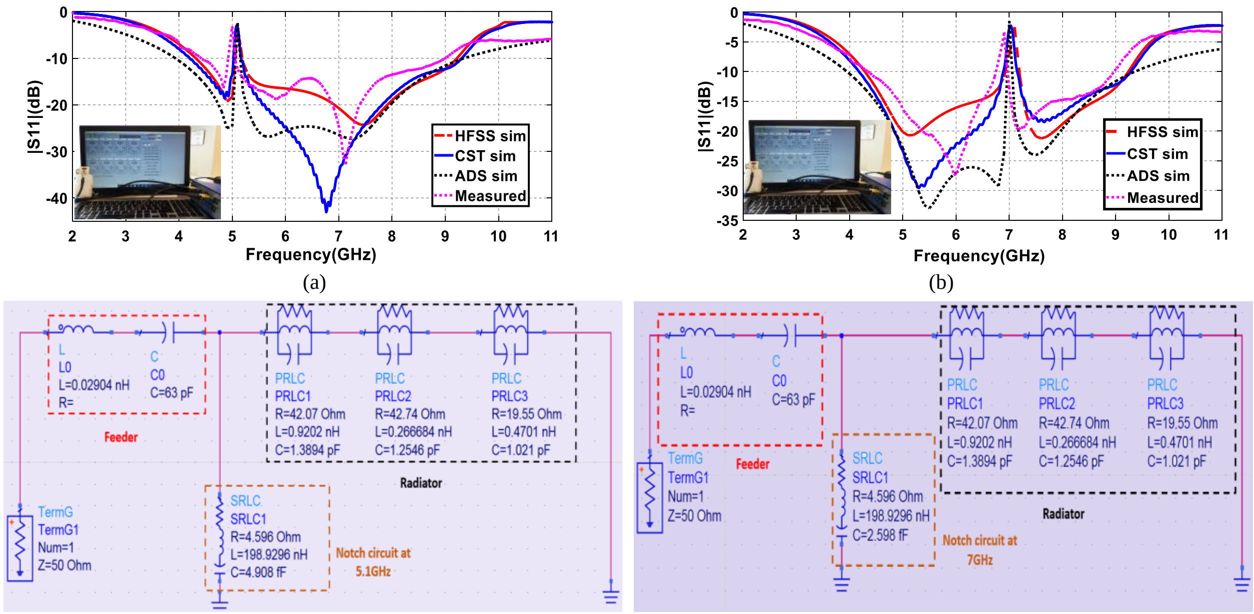

(c) (d)

Fig. 17. Simulated, equivalent circuit model and measured reflection coefficient results for: (a) first WLAN notch (5.1GHz) and (b) fourth Wi-Fi 6E notch (7.02GHz). And the proposed antenna equivalent circuit model for: (c) WLAN notch (*F*=5.1GHz); (d) Wi-Fi 6E notch (*F*=7GHz).

TABLE II: COMPARISON OF THE PROPOSED NOTCHED ANTENNA WITH EXISTING ANTENNAS IN THE LITERATURE

Ref.	Antenna Size (mm^2)	Substrate (ε_r, *h* in mm)	Bandwidth (GHz)	Notch frequencies or notch bands (GHz)	Reconfigurable Notch	Max Gain (dBi)
[2]	20×26	FR4- ε_r=4.4, *h*=1.6	2.4-10.5	3.2-3.9, 5.1-5.85	No	7
[7]	11.5×14.5	FR4- ε_r=4.4, *h*=1.5	2.2-14	3.4-3.7, 5.2-5.8	No	4.1
[8]	26×27	FR4- ε_r=4.4, *h*=1.6	2.19-13.95	4.67-6.21	No	5
[10]	24×12	RT/Duroid 5880- ε_r=2.2, *h*=0.787	3.1-11	3.5, 5.5	No	4.1
[12]	31×40	Roger 3010-ε_r=10.2, *h* = 0.635	3 -10.28	4.5-5.38	No	6.2
[13]	25×33	ε_r =2.2, 1.14	3.04 – 11.31	3.37- 3.80, 4.26 -5.85 ,7.25 -8.81	No	6
[14]	24×36	RO4003TM-ε_r =3.38, *h* = 1.524	3-12	5.15-5.825, 5.15–5.35, 5.725–5.825	No	5
[15]	24×30	FR4 -ε_r =4.4, *h* =1	2.6-12	3.3–4, 5.15–5.4, 5.8–6.1	No	5.5
[16]	24×12	RT/Duroid 5880-ε_r =2.2, 0.787	3.1-11	3.5, 5.5	Yes	3.5
[17]	33×21	FR4-ε_r =4.3, *h* =1.6	3-10.6	3.3-3.7, 5-5.30	Yes	6
[19]	35×35	RT/Duroid 5880- ε_r =2.2, *h* =1.575	3.1-12	3.8, 5.7	Yes	5.5
[20]	48×55	FR4-ε_r =4.4, *h* =1.5	1.9-12	3.8, 5.5	Yes	Not mentioned
[21]	30×40	Rogers (RO4350B) -ε_r =3.66, *h* =0.76	2-8	3, 6.8	Yes	6.8
[22]	46×52	FR4-ε_r =4.4, *h* =1.6	2.2-8.4	3.42 - 3.82, 5.17- 6.07, 6.89 -7.48 (OFF-OFF State)	Yes	4.5
[23]	24×30.5	RO4003C-ε_r =3.38, *h* =1.5	2.5-10.5	3.5 and in between 5.45-5.9	Yes	5
Proposed Work	25×28	RO4003C-ε_r =3.38, *h* = 0.81	4.2-9.2	In between (5.15-5.35) or (5.725-5.825) or (5.925-7.125)	Yes	4

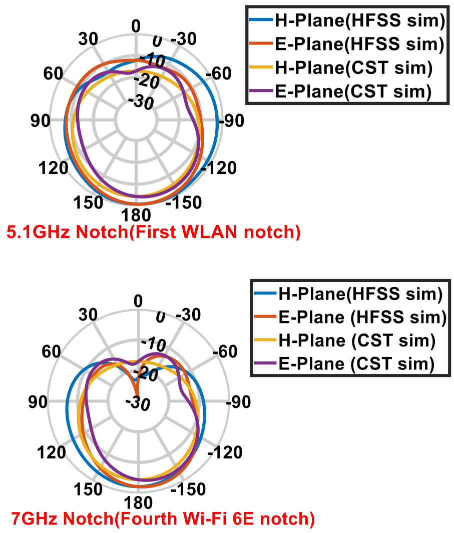

Fig. 18. Simulated radiation patterns for the notched antenna.

VI. Conclusion

In this paper, a compact monopole antenna with switchable WLAN or Wi-Fi 6E band-notched is presented. By adding two resonator conductors beside to the basic antenna feeder, the unwanted frequency can be rejected based on the conductor resonator length. A group of PIN diodes are used to control resonator conductor length, where the ON/OFF states for the diodes are controlled by a diodes switch matrix box. The CST and HFSS simulations results are in a good agreement with measurement results, where a small deviation is presented that due to fabrication tolerance and mismatch in SMA connectors. Also, the design of the proposed antenna is compact and suitable for C-band applications with no interferences by Wi-Fi 6E or WLAN services.

Conflict of Interest

The authors declare no conflict of interest.

Author Contributions

Under the supervision of Prof Ashraf S. Mohra, Asst. Prof. Abdelhady M. Abdelhady, and Dr Hesham A. Mohamed, Samar A. Refaat has conducted and wrote the paper; all authors had approved the final version.

References

[1] Z. J. Tang, X. F. Wu, and J. Zhan, "Novel compact band-notched UWB antenna using convex-shaped slot patch," *Microw. Opt. Technol. Lett.*, vol. 57, no. 1, pp. 201–203, 2015.

[2] R. K. Garg, M. V. D. Nair, S. Singhal, and R. Tomar, "A miniaturized ultra-wideband antenna using "modified" rectangular patch with rejection in WIMAX and WLAN bands," *Microw. Opt. Technol. Lett.*, vol. 63, pp.1271-1277, Nov. 2020.

[3] R. Chandel, A. K Gautam, and K. Rambabu, "Tapered fed compact UWB MIMO-diversity antenna with dual band-notched characteristics," *IEEE Trans. Antennas Propag.*, vol. 66, no. 4, pp. 1677–1684, 2018.

[4] A. K. Gautam, S. Yadav, and K. Rambabu, "Design of ultra-compact UWB antenna with band-notched characteristics for MIMO applications," *IET Microw. Antennas Propag.*, vol. 12, no. 12, pp. 1895–1900, 2018.

[5] W. X Chen, C. H. Lee, and C. I. G Hsu, "CM suppression enhancement for balanced band-notched UWB closed-aperture antenna," *Electronics Letters.*, vol. 53, no. 19, pp. 1291–1292, 2017.

[6] S. U Rehman and M. A. S Alkanhal, "Design and system characterization of ultra-wideband antennas with multiple band-rejection," *IEEE. Access*, vol. 5, pp.17988–17996, June 2017.

[7] K. S. Sultan, O. M. A. Dardeer, and H. A. Mohamed, "Design of compact dual notched self-complementary UWB antenna," *Open Journal of Antennas and Propagation*, vol. 5, pp. 99-109, Sep. 2017.

[8] R. K. Garg, M. V. D. Nair, S. Singhal S, and R. Tomar, "A new type of compact ultrawideband planar fractal antenna with WLAN band rejection," *Microw. Opt. Technol Lett.*, vol. 62, pp. 2537–2545, Feb. 2020.

[9] I. B, Vendik, A. Rusakov, K. Kanjanasit, J. Hong, and D. Filonov, "Ultrawideband (UWB) planar antenna with single-, dual-, and triple-band notched characteristic based on electric ring resonator," *IEEE Antennas Wireless Propag. Lett.*, vol. 16, pp. 1597-1600, Jan. 2017.

[10] H. Yang, X. Xi, Y. Zhao, L. Wang, and X. Shi, "A compact filtering UWB antenna with band-notched function," *IEICE Electron. Express*, vol. 15, no. 12, 2018.

[11] X. L. Liu, Y. Z. Yin, P. A. Liu, J. H. Wang, and B. A. Xu, "A CPW-fed dual band-notched UWB antenna with a pair of bended dual-L-shape parasitic branches," *Progress in Electromagnetic Research*, vol. 136, pp. 623-634, Jan. 2013.

[12] J. R. Kelly, P. S. Hall, and P. Gardner, "Band-notched UWB antenna incorporating a microstrip open-loop resonator," *IEEE Trans. on Antennas and Propagation*, vol. 59, no. 8, pp. 3045–3048, Aug. 2011.

[13] Y. Sung, "Triple band-notched UWB planar monopole antenna using a modified H-shaped resonator," *IEEE Trans. on Antennas and Propagation*, vol. 61, no. 2, pp. 953-957, 2013.

[14] K. S. Ryu and A. A. Kishk, "UWB antenna with single or dual band-notches for lower WLAN band and upper WLAN band," *IEEE Trans. on Antennas and Propagation*, vol. 57, no. 12, pp. 3942–3950, 2009.

[15] X. J. Liao, H. C. Yang, N. Han, and Y. Li, "Aperture UWB antenna with triple band-notched characteristic," *Electronics Letters*, vol. 47, no. 2, pp. 77-79, 2011.

[16] H. Yang, X. Xi, H. Hou, Y. Zhao, and Y. Yuan, "Design of reconfigurable filtering ultra-wideband antenna with switchable band-notched functions," *Int. Journal of Microwave and Wireless Technologies*, vol. 10, no. 9, pp. 1065–1071, 2018.

[17] H. Medkour, M. Cheniti, A. Narbudowicz, S. Das, E. Vandelle, and T. Vuong, "Coplanar waveguide-based ultra-wide band antenna with switchable filtering of WIMAX 3.5GHz and WLAN 5GHz signals," *Microw. Opt. Technol. Lett.*, vol. 62, pp. 2398–2404, Feb. 2020.

[18] H. Yang, X. Xi, Y. Zhao, Y. Tan, Y. Yuan, and L. Wang, "Compact slot antenna with enhanced band edge selectivity and switchable band-notched functions for UWB applications," *IET Microwaves, Antennas & Propagation*, vol. 13, no. 7, pp. 982-990, 2019.

[19] W. A. E. Ali, H. A. Mohamed, A. A. Ibrahim, and M. Z. M. Hamdalla, "Gain improvement of tunable band-notched UWB antenna using metamaterial lens for high speed wireless communications," *Microsystem Technologies*, vol. 25, pp. 4111–4117, Jan. 2019.

[20] A. A. Al-Behadili, A. R. Azeez, S. Ahmed, and Z. A. Abdul Hassain, "Design of ultra-wideband tapered slot patch antenna with reconfigurable dual band-notches," *Journal of Southwest Jiaotong University*, vol. 55, no. 4, pp. 1-7, Aug. 2020.

[21] H. Ayadi, J. Machac, S. Beld, and L. Latrach, "Planar hexagonal antenna with dual reconfigurable notched bands for wireless communication devices," *Radioengineering*, vol. 30, no. 1, pp. 25-32, Apr. 2021.

[22] R. Orugu and N. Moses, "Triangular fractal loaded reconfigurable antenna with notch band characteristics," *Int. Journal of*

Numerical Modelling Electronic Networks Devices and Fields, vol. 34, no. 1, pp. 1-11, Sep. 2020.

[23] A. Haider, M. Rahman, H. Ahmad, M. N. Jahromi, M. T. Niaz, and H. S. Kim, "Frequency-agile WLAN notch UWB antenna for URLLC applications," *Computers, Materials & Continua*, vol. 67, no. 2, pp. 2243-2254, 2021.

[24] FCC Adopts New Rules for the 6GHz Band, Unleashing 1,200 Megahertz of Spectrum for Unlicensed Use, Federal Communications Commission, April 23, 2020.

[25] Report and Order-Unlicensed Use of the 6GHz Band, Expanding Flexible Use in Mid-Band Spectrum between 3.7 and 24GHz, Federal Communications Commission, FCC-20-51, April 24, 2020.

[26] H. A. Mohamed, A. S. Elkorany, S. A. Saad, and D. A. Saleeb, "New simple flower shaped reconfigurable band-notched UWB antenna using single varactor diode," *Progress in Electromagnetics Research C*, vol. 76, pp. 197–206, Aug. 2017.

[27] K. Molugaram and G. S. Rao, *Statistical Techniques for Transportation Engineering*, 1st ed, Butterworth-Heinemann, Elsevier, 2017, ch. 5, pp. 281-287.

[28] K. H. Sayidmarie and L. S. Yahya, "Modeling of dual-band crescent-shape monopole antenna for WLAN applications," *Int. Journal of Electromagnetics and Applications*, vol. 4, no. 2, pp. 31-39, 2014.

Samar Ahmed Refaat was born in Egypt in 1989. She received the B.Sc. degree in electronics and communications from Benha Faculty of Engineering in 2011 and the M.Sc. degree in 2017 from Benha University, Egypt. She is currently a teaching assistant at Benha Faculty of Engineering, Benha University, Egypt and pursuing the Ph.D. degree. Her current research interest in reconfigurable microstrip antennas.

Hesham Abdelhady Mohamed received his B.Sc. degree in Electronics and communication engineering from the University of Menofia in 2003 and received his M.Sc. and Ph.D. degree from Ain Shams University in 2009 and 2014, respectively. He is currently Associate Researcher at Electronics Research Institute (ERI), Giza, Egypt and he is a member of the IEEE (Institute of Electrical and Electronic Engineers). His research interests on microwave circuit designs, planar antenna systems, recently on EBG structures, UWB components and antenna and RFID systems, radar Absorbing materials, energy harvesting and wireless power transfer, smart antennas, microstrip antennas, microwave filters, Metamaterials, and MIMO antennas and its applications in wireless communications.

Abdelhady Mahmoud Abdelhady received the B.Sc. (Hons.), M.Sc., and Ph.D. degrees, in 2000, 2005, and 2013, respectively. From 2010 to 2012, he was a Ph.D. Researcher with the State Key Laboratory of Millimeter-Wave, Nanjing, China. From 2013 to 2015, he was a Post-Doctoral Fellow with Concordia University, Montreal, QC, Canada. He is currently an Associate Professor with the Faculty of Engineering, Department of Electrical Engineering, Benha University. His current research interests include the design of RFID passive tags, artificial lens, circularly polarized, and linearly polarized reflectarrays and transmitarrays, MIMO, 3D printed structure, broadband circularly polarized dielectric resonator antennas and polarizer twisting structures at microwave and millimeter wave frequencies.

Ashraf Shouki Seliem Mohra was born in Egypt in 1963. He received the B.Sc. degree in Electronics and communications from Shoubra Faculty of Engineering in 1986. He received the M.Sc. and Ph.D. degree in Electronics and communications from Ain Shams University, Cairo, Egypt, in 1994 and 2000, respectively. He is currently professor of Electrical Engineering, at Benha Faculty of Engineering, Benha University, Egypt. His current research interests include microstrip antennas, filters, couplers, Hybrid junctions, computer aided design of planar and uniplanar of MIC's and MMIC's, Non-destructive techniques, Metamaterials and defected ground struct.